flat plate boundary layer. It is of the order of the probe diameter. In laminar incompressible boundary layers, the displacement thickness δ^* of an axisymmetric paraboloid is[6]

$$(\delta^*/x) = 0\{1/[(Re_x)ei(Re_L)]^{1/2}\}$$

where L is the focal length, x the distance from the tip of the body, and

$$ei(Re_L) = \int_{Re_L}^{\infty}\left[\frac{(e^{-\eta})}{\eta}\right]d\eta \cong -0.5772 + \ln\left(\frac{1}{Re_L}\right) + Re_L - \left(\frac{Re_L^2}{2\cdot 2!}\right) + \ldots$$

for small Reynolds numbers Re_L. This relation shows that the smaller the L, and therefore the smaller the diameter, the smaller is the ratio of displacement thickness δ^* to x. This behavior of δ^* seems to be one essential cause of the comparatively small interaction results obtained. To obtain a more detailed understanding of the flow field, additional theoretical and experimental investigations are necessary. However, the present results can be used for the reduction of static pressure measurements, obtained using static probes similar to the one given in Fig. 1.

References

[1] Matthews, M. L., "An experimental investigation of viscous effects on static and impact pressure probes in hypersonic flow," Graduate Aeronaut. Labs., Calif. Inst. Tech., Hypersonic Research Project, Memo. 44 (June 2, 1958).

[2] Hayes, W. D. and Probstein, R. F., *Hypersonic Flow Theory* (Academic Press, New York and London, 1959), Chap. IX.

[3] Talbot, L., Koga, T., and Sherman, P. M., "Hypersonic viscous flow over slender cones," NACA TN 4327 (September 1958).

[4] Clippinger, R. F., Giese, T. H., and Carter, W. C., "Tables of supersonic flows about cone cylinders. Part I: Surface data," Ballistic Res. Labs. Rept. 729 (October 15, 1960).

[5] Timman, K., "Hypersonic flow about a thin body of revolution," AGARD Rept. 141 (July 1957).

[6] Mark, R. M., "Laminar boundary layers on slender bodies of revolution in axial flow," Graduate Aeronaut. Labs., Calif. Inst. Tech., Hypersonic Research Project, Memo. 21 (July 30, 1954).

Gyro Torquing Signals at an Arbitrary Azimuth on an Ellipsoidal Earth

Myron Kayton*

Litton Industries, Woodland Hills, Calif.

THIS note shows the exact expressions for gyro torquing signals in a wander-azimuth system. It is not intended as a general discussion of wander-azimuth mechanizations. The use of a wandering azimuth requires special computation provisions for generating α.

Consider a vehicle at P, Fig. 1, moving near the surface of the earth at a velocity $\bar{V}$ (not necessarily horizontal). The arc DCE is a worldwide reference ellipsoid representing the earth, and $ABCP$ is the normal to the ellipsoid which passes through P. $CP = h$ is the height of the vehicle above the ellipsoid, and ϕ is the geographic latitude of the vehicle. The relevant dimensions of the ellipsoid are its semimajor axis a and its eccentricity ϵ [not to be confused with the flattening or ellipticity, $f = 1 - (1 - \epsilon^2)^{1/2} \approx \epsilon^2/2$].

Received September 3, 1963.

* Senior Research Engineer, Guidance and Control Systems Division. Member AIAA.

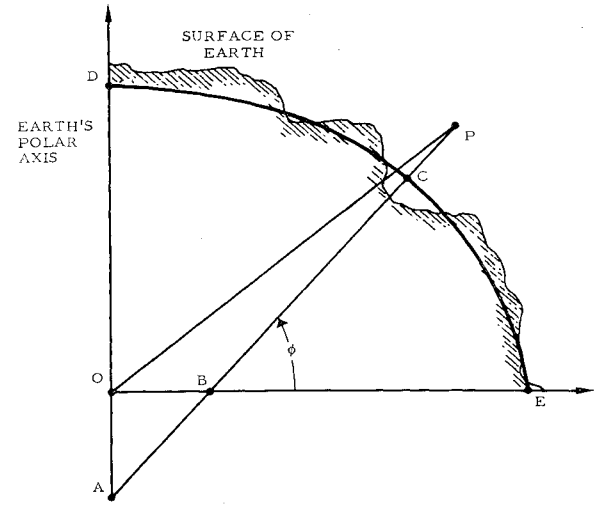

Fig. 1 Meridian section of reference ellipsoid.

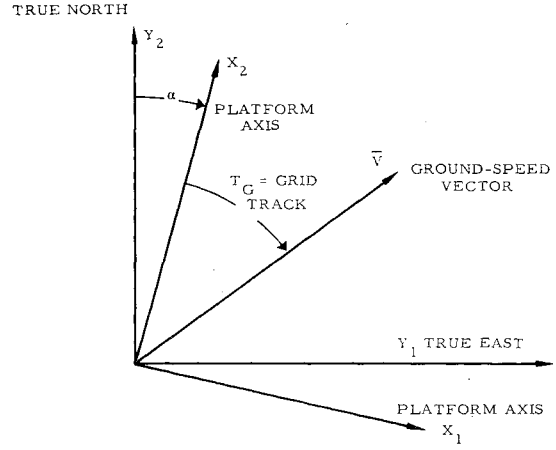

Fig. 2 Plan view of level platform at an azimuth α.

The vehicle is assumed to carry an inertial platform whose orthogonal torquer axes define the coordinate frame $x_1x_2x_3$. The platform is locally level (x_3 lies along $ABCP$ and points upward) and oriented with its x_2 axis at an azimuth α from north (Fig. 2). A horizontal plane at any altitude is here defined as a plane perpendicular to the projected normal to the ellipsoid, $ABCP$.

A non-north azimuth orientation is used for many purposes:

1) It can allow the use of a transverse pole, on the earth's equator, to permit operation near the true poles.

2) It can allow the use of redundant coordinates, such as direction cosines, to permit operation at all latitudes.

3) It can eliminate the Coriolis correction or maintain a constant azimuth torque rate, independent of vehicle speed.

The basic mechanization equations for an aircraft or ship inertial navigator are[1]

$$d\bar{V}/dt]_p = \bar{f} + (\bar{\omega}_{EP} + 2\bar{\Omega}) \times \bar{V} - g \qquad (1)$$

where

$\bar{f}$ = accelerometer output, expressed as an acceleration

$\bar{\omega}_{EP}$ = desired angular velocity of platform relative to the earth

$\bar{\Omega}$ = earth's inertial angular velocity

$d\bar{V}/dt]_p$ = time derivative of $\bar{V}$ in platform axes

$\bar{g}$ = gravity (not Newtonian gravitation $\bar{G}$). The horizontal component of $\bar{g}$ (tangent to the reference ellipsoid) is zero, neglecting local anomalies, at all altitudes below 35 naut miles

These equations can be used to determine the horizontal components of $\bar{V}$, Vx_1, and Vx_2 in terms of accelerometer outputs and the desired platform torque rates. These torque rates, which must also be supplied to the gyro torquers, can be computed as follows.

Define the east, north, and vertical axes, y_1, y_2, and y_3, respectively, as in Fig. 2. The axes of y_1 and y_2 are principal directions of curvature on the ellipsoid (east and north). The components of ω_{EP} rates in principal axes are

$$\left.\begin{aligned}\omega_{y_1} &= -V_{y_2}/(\rho_m + h)\\ \omega_{y_2} &= V_{y_1}/(\rho_p + h)\end{aligned}\right\} \tag{2}$$

where

ρ_m = principal radius of curvature of the reference ellipsoid in the meridian plane, sometimes written as ρ, i.e., $\rho_m = a(1 - \epsilon^2)/(1 - \epsilon^2 \sin^2\phi)^{3/2}$

ρ_p = principal radius of curvature in the vertical east-west plane, called the prime radius of curvature and sometimes written as η, i.e., $\rho_p = a/(1 - \epsilon^2 \sin^2\phi)^{1/2}$

By resolving these equations into platform axes and performing some algebraic manipulation,

$$\left.\begin{aligned}\omega_{x_1} &= \frac{-V_{x_2}}{\rho_\alpha + h} + \frac{V_{x_1}\sin 2\alpha}{2}\,\frac{\rho_\rho - \rho_m}{(\rho_\rho + h)(\rho_m + h)}\\ \omega_{x_2} &= \frac{V_{x_1}}{\rho_{\alpha+90} + h} - \frac{V_{x_2}\sin 2\alpha}{2}\,\frac{\rho_\rho - \rho_m}{(\rho_\rho + h)(\rho_m + h)}\end{aligned}\right\} \tag{3}$$

where

ρ_α = radius of curvature at an azimuth $\alpha(1/\rho_\alpha) = (\sin^2\alpha/\rho_\rho) + (\cos^2\alpha/\rho_m)$

$\rho_{\alpha+90}$ = radius of curvature at an azimuth $\alpha + 90°$

$\rho_\rho - \rho_m = (a\epsilon^2 \cos^2\phi)/(1 - \epsilon^2 \sin^2\phi)^{3/2}$
$= [\epsilon^2/(1 - \epsilon^2)]\rho_m \cos^2\phi$

Equations (3) are the exact expressions for the torque rates of the platform relative to earth. The inertial torque rate is $\bar{\omega}_{EP} + \bar{\Omega} = \bar{\omega}_{IP}$. These are not power series approximations.

Note that the torque rate about the x_1 axis is not merely the x_2 component of velocity divided by the radius of curvature in the $x_2 - x_3$ plane except at cardinal headings. At all other headings, a small correction, proportional to V_{x1}, must be added. This correction is of the order $(\epsilon^2/2)(V/a)$, or about 0.1 deg/hr at 1800 knots. In geometric terms, the platform rotates around the velocity vector as well as around the binormal.

Equations (3) can be expanded in a power series in (h/a) and ϵ, which is accurate to $10^{-4}\,\Omega(0.0015$ deg/hr) for speeds up to 1800 knots and at altitudes below 25 naut miles:

$$\left.\begin{aligned}\omega_{x_1} &= -\frac{V_{x_2}}{a}\left[1 - \frac{h}{a} - \epsilon^2\left(\frac{\sin^2\phi}{2} - \cos^2\phi\cos^2\alpha\right)\left(1 - \frac{2h}{a}\right)\right] + \frac{V_{x_1}}{a}\frac{\epsilon^2}{2}\sin 2\alpha\cos^2\phi\\ \omega_{x_2} &= \frac{V_{x_1}}{a}\left[1 - h/a - \epsilon^2\left(\frac{\sin^2\phi}{2} - \cos^2\phi\sin^2\alpha\,(1 - 2\frac{h}{a})\right)\right] - \frac{V_{x_2}}{a}\frac{\epsilon^2}{2}\sin 2\alpha\cos^2\phi\end{aligned}\right\} \tag{4}$$

The calculation of position from the three components of velocity, as found in Eq. (1), depends on the coordinate frame chosen. For example, if $\alpha = 0$ so that the platform is north-seeking, then the latitude ϕ and longitude λ can be found from

$$\phi = \int_0^t \frac{V_{x_2}}{\rho_m + h}\,dt$$

$$\lambda = \int_0^t \frac{V_{x_1}}{(\rho_\rho + h)\cos\phi}\,dt$$

References

[1] Pitman, G. R. (ed.), *Inertial Guidance* (John Wiley and Sons Inc., New York, 1962), p. 149.

Shock Detachment Distance for Blunt Bodies in Argon at Low Reynolds Number

A. B. Bailey* and W. H. Sims†
ARO Inc., Arnold Air Force Station, Tenn.

Nomenclature

M_∞ = freestream Mach number
R_b = body radius (≡ nose radius of curvature for a sphere)
Re_2 = Reynolds number based on body diameter and conditions immediately downstream of a normal shock
T_0 = reservoir temperature of gas
T_w = body wall temperature
Δ = shock detachment distance measured from the body to the shock leading edge along the axis of symmetry

THE shock detachment distance in front of blunt bodies at high Reynolds numbers has been studied both theoretically and experimentally. Van Dyke and Gordon[1] have presented a theoretical analysis for a series of perfect gases having specific heat ratios of 1, $\frac{7}{5}$, and $\frac{5}{3}$ and a Mach number range from 1.2 to infinity. For a sphere, their analysis indicates that the shock detachment distance is primarily a function of the density ratio across the normal part of the shock. In such studies, it is implied that the shock and boundary-layer thicknesses are small compared with the shock detachment distance. At low Reynolds numbers the shock and boundary-layer thicknesses are no longer negligible, and at sufficiently low Reynolds numbers the shock and boundary layers merge. This implies that there must be a Reynolds number below which the shock detachment distance becomes a function of Reynolds number as well as density ratio.

Probstein and Kemp,[2] Ho and Probstein,[3] and Levinsky and Yoshihara,[4] among others, have analyzed this problem. All of these analyses indicate that as the fully merged regime is approached the shock detachment distance increases to a value greater than the inviscid value.

The low-density, hypervelocity (LDH) wind tunnel,[5] in operation at the von Kármán Gas Dynamics Facility of the Arnold Engineering Development Center, is well suited for low Reynolds number shock detachment distance investigations. When this tunnel is operated using argon, there is a natural flow visualization thought to be caused by radia-

Received September 3, 1963. This work was sponsored by Arnold Engineering Development Center, Air Force Systems Command, U. S. Air Force, under Contract No. AF 40(600)-1000.

* Engineer, Research Branch, von Kármán Gas Dynamics Facility.

† Engineer, Research Branch, von Kármán Gas Dynamics Facility. Member AIAA.